BIOCHEMISTRY
including biophysical chemistry & molecular biology

Article

pubs.acs.org/biochemistry

Pectin–Cellulose Interactions in the *Arabidopsis* Primary Cell Wall from Two-Dimensional Magic-Angle-Spinning Solid-State Nuclear Magnetic Resonance

Tuo Wang,[†] Olga Zabotina,[‡] and Mei Hong*[,†]

[†]Department of Chemistry and Ames Laboratory, Iowa State University, Ames, Iowa 50011, United States

[‡]Department of Biochemistry, Biophysics, and Molecular Biology, Iowa State University, Ames, Iowa 50011, United States

Supporting Information

ABSTRACT: The primary cell wall of higher plants consists of a mixture of polysaccharides whose spatial proximities and interactions with each other are not well understood. We recently obtained the first two-dimensional (2D) and three-dimensional high-resolution magic-angle-spinning ^{13}C solid-state nuclear magnetic resonance spectra of the uniformly ^{13}C-labeled primary cell wall of *Arabidopsis thaliana*, which allowed us to assign the majority of ^{13}C resonances of the three major classes of polysaccharides: cellulose, hemicellulose, and pectins. In this work, we measured the intensity buildup of $^{13}C-^{13}C$ cross-peaks in a series of 2D ^{13}C correlation spectra to obtain semiquantitative information about the spatial proximities between different polysaccharides. Comparison of 2D spectra measured at different spin diffusion mixing times identified intermolecular pectin–cellulose cross-peaks as well as interior cellulose–surface cellulose cross-peaks. The intensity buildup time constants are only modestly longer for cellulose–pectin cross-peaks than for interior cellulose–surface cellulose cross-peaks, indicating that pectins come into direct contact with the cellulose microfibrils. Approximately 25–50% of the cellulose chains exhibit close contact with pectins. The ^{13}C magnetization of the wall polysaccharides is not fully equilibrated by 1.5 s, indicating that pectins and cellulose are not homogeneously mixed on the molecular level. We also assigned the ^{13}C signals of cell wall proteins, identifying common residues such as Pro, Hyp, Tyr, and Ala. The chemical shifts indicate significant coil and sheet conformations in these structural proteins. Interestingly, few cross- peaks were observed between the proteins and the polysaccharides. Taken together, these data indicate that the three major types of polysaccharides in the primary wall of *Arabidopsis* form a single cohesive network, while structural proteins form a relatively separate domain.

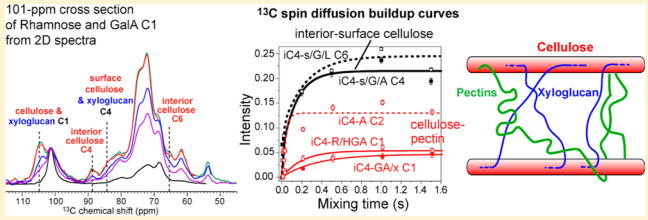

The plant cell wall (CW) is a polysaccharide-rich insoluble material that shapes plant cell morphology, maintains ionic balance, shields plant cells from environmental stress, and allows plant cell growth. These functions are conducted by the polysaccharides and proteins in the CW, whose three-dimensional structures and packing have largely evaded high-resolution characterization because of the insoluble and amorphous nature of the CW biopolymers. The primary cell walls of young growing plants contain three main classes of polysaccharides: cellulose, hemicellulose, and pectins.[1−4] Cellulose consists of β-1,4-linked glucan chains and is organized into microfibrils that are 3–5 nm in diameter[5] in the primary wall. Hemicellulose and pectins comprise the matrix surrounding the cellulose microfibrils. Hemicellulose is operationally defined as the alkali-extracted fraction of the cell wall that interacts strongly with cellulose. In dicotyledonous plants, the main hemicellulose is xyloglucan (XG), which consists of a β-1,4-glucose (Glc) backbone substituted at regular positions with α-D-xylose (Xyl). Some Xyl units are further substituted with β-D-galactose (Gal) and α-L-fucose (Fuc). Pectins are anionic polysaccharides rich in α-D-galacturonic acid (GalA) residues. In *Arabidopsis thaliana*, the main pectins include homogalacturonan (HGA), which are linear chains of 1,4-α-D-GalA (GA), rhamnogalacturonan (RG) I, and RG II. RG I consists of a backbone of alternating 1,4-α-D-GalA and 1,2-α-L-rhamnose (Rha) units, the latter often decorated with homopolymeric side chains of β-D-Gal and α-L-arabinose (Ara).[6] HGA and RG I contain significant methyl esterification and O-acetylation. Demethylation of HGA yields negatively charged carboxyl groups, which bind divalent Ca^{2+} to form cross-linked HGA chains.[7] RG II is a highly substituted pectin that tends to self-associate via boron. Pectins have diverse functions such as regulating cell wall porosity, modulating pH and ionic balance, and controlling cell–cell adhesion and cell signaling.[7]

In addition to polysaccharides, proteins also constitute an important structural component of the primary cell wall. The main structural proteins include hydroxyproline (Hyp)-rich glycoproteins (HRGPs), glycine-rich proteins (GRPs), proline-rich proteins (PRPs), and arabinogalactan proteins (AGPs).[8] The first three groups of structural proteins are highly enriched

Received: November 18, 2012
Revised: November 19, 2012
Published: November 20, 2012

in a small number of amino acids in repetitive sequences, while AGPs are predominantly (~90%) carbohydrates attached to a small amount (~10%) of protein. Although the exact abundance of each structural protein depends on the cell type, on the basis of the amino acid compositions of these glycoproteins, the most common amino acid residues in the cell wall are Gly, Hyp, Lys, Pro, Ala, and Tyr.[8] Little secondary structure information is available so far for these structural proteins. One of the better-studied CW proteins is extensin, a HRGP with a Ser-$(Hyp)_4$ repeat sequence.[9,10]

Structure investigation of plant cell walls so far has mainly involved compositional analysis of monosaccharides after chemical extraction of the wall components and imaging of the crystalline cellulose core by electron microscopy and X-ray scattering. The extraction-based chemical analysis suffers from destruction or alteration of the chemical and physical interactions among polysaccharides, while microscopy and diffraction studies cannot characterize the amorphous matrix polysaccharides well. Solution nuclear magnetic resonance (NMR) has been used to study solubilized cell walls,[11,12] but with the similar limitation of cleaving some of the chemical bonds. Thus, molecular-level structural information about the polysaccharides in intact plant CWs has remained scarce.[3,13,14]

We recently demonstrated the feasibility of using multidimensional magic-angle-spinning (MAS) solid-state NMR (SSNMR) spectroscopy to investigate the structure, dynamics, and intermolecular interactions of polysaccharides in intact plant CWs under near-native conditions.[15] By labeling whole *A. thaliana* plants with ^{13}C during growth, we obtained sufficient sensitivity to detect and correlate the signals of all carbons in the CW polysaccharides. The plants were treated mildly to remove only intracellular proteins, small molecules, starch, and lipids, while retaining alcohol-insoluble residues that belong to the CW. The two-dimensional (2D) and three-dimensional (3D) ^{13}C correlation MAS spectra allowed the assignment of the structurally informative ^{13}C isotropic chemical shifts of most CW polysaccharides. The 3D NMR spectra revealed cross-peaks between different polysaccharides, giving the first glimpse of the spatial proximity of wall polysaccharides on the molecular level. We also used this multidimensional SSNMR approach to characterize the CW structural and dynamical changes in several *Arabidopsis* mutants that are defective in xyloglucan synthesis[15] and cellulose synthesis.[16]

The previous 3D $^{13}C-^{13}C-^{13}C$ correlation spectra of wild-type CW revealed a number of pectin−cellulose cross-peaks, suggesting that HGA and RG I contact the cellulose microfibrils. This finding challenged the prevailing model of plant CW structure, in which pectic polysaccharides were thought to form a network separate from the cellulose−hemicellulose network.[2,17,18] In the present study, we extract more quantitative information about pectin−cellulose proximities by measuring cross-peak intensities as a function of spin diffusion mixing time in a series of 2D correlation spectra. The simplicity of measuring 2D spectra compared to 3D spectra allows us to detect cross-peaks at multiple mixing times and to significantly extend the maximal mixing time, thus probing much longer distances than before. The absence of cross-peaks at short mixing times and the presence at long mixing times give unambiguous indications of the long-range nature of some correlation peaks. By comparing the spin diffusion buildup times of cellulose−pectin, cellulose−cellulose, and pectin−pectin cross-peaks, we can obtain information about the relative proximity between different polysaccharides. In addition, we have assigned the ^{13}C signals of structural proteins to obtain information about the backbone conformation of these proteins and their spatial proximities with the polysaccharides in the intact CW.

MATERIALS AND METHODS

Plant Material. The uniformly ^{13}C-labeled wild-type *A. thaliana* primary cell wall was prepared as described previously.[15] Briefly, plants were germinated and grown in the dark in a liquid culture where the only carbon source was uniformly ^{13}C-labeled glucose (5 g/L). Glucose was chosen because it is readily available in many ^{13}C-labeled forms, and it is also one of the most direct carbon precursors of plants. It can be converted to UDP-glucose and other sugar nucleotides, which are used by plant cells for polysaccharide biosynthesis.[6] Whole seedlings were harvested, powdered, and homogenized. After centrifugation at 12000*g* for 20 min, small cytoplasmic molecules were removed along with the supernatant. The pellet was washed with a chloroform/methanol (1:1) solution to remove nonpolar compounds. Dry alcohol-insoluble residues were suspended in 50 mM sodium acetate buffer (pH 5.2) containing 1.5% SDS and 5 mM sodium metabisulfate to remove most intracellular proteins and low molecular-weight compounds. Starch was removed using α-amylase. On the basis of quantitative ^{13}C spectra, the treated CW contains mostly polysaccharides and proteins and has negligible lignin. Approximately 30 mg of CW material was hydrated to 45% (w/w) in pH 7.5 phosphate buffer and packed into a 4 mm MAS rotor for experiments on a 600 MHz NMR instrument. Approximately 10 mg of CW was packed into a 2.5 mm rotor for experiments on a 900 MHz NMR spectrometer.

To examine the extent of structural similarity between dark-grown CW and light-grown CW, we grew two unlabeled *Arabidopsis* plants in light versus dark for 10 days. The light-grown plant was predominantly composed of short hypocotyls with first primary leaves, while the dark-grown sample exhibited elongated hypocotyls. The plant material was homogenized in 0.1 M phosphate buffer (pH 7) using a mortar and pestle, and solid tissues were collected by centrifugation at 13000 rpm for 20 min. The resulting homogenized tissues, dark green for the light-grown sample and light yellow for the dark-grown sample, were packed into 4 mm MAS rotors.

Solid-State NMR Experiments. Most ^{13}C NMR spectra were measured at magnetic fields of 14.1 and 21.1 T, corresponding to ^{1}H Larmor frequencies of 600 and 900 MHz, respectively. On the 600 MHz NMR instrument, the typical radiofrequency (rf) field strengths were 62−75 kHz for ^{1}H decoupling and 50 kHz for ^{13}C pulses. All ^{13}C chemical shifts were reported on the TMS scale using the ^{13}CO chemical shift of α-glycine at 176.465 ppm as an external reference, which corresponds to an adamantane CH_2 chemical shift of 38.48 ppm.

A series of ^{1}H-driven ^{13}C spin diffusion (PDSD) experiments were conducted on the 600 MHz NMR instrument using a 4 mm MAS probe. The spin diffusion mixing times ranged from 5 ms to 1.5 s to probe increasing internuclear distances. Initial transverse ^{13}C magnetization was created by $^{1}H-^{13}C$ cross-polarization (CP) with a contact time of 700 μs. The MAS frequency was 8 kHz, and the temperature was 253 K, based on thermocouple-reported values.

Double-quantum (DQ) filtered 2D correlation spectra were measured to identify short-range cross-peaks. The SPC5 sequence[19] was used to recouple the $^{13}C-^{13}C$ dipolar coupling

dx.doi.org/10.1021/bi3015532 | *Biochemistry* 2012, 51, 9846−9856

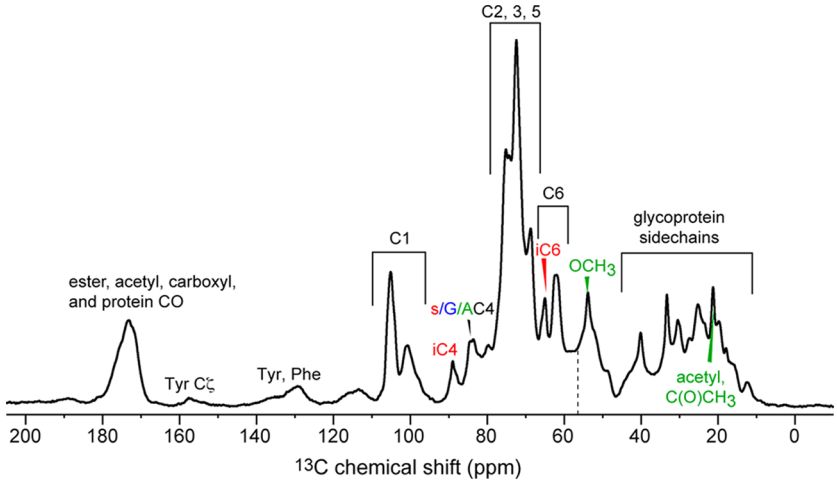

Figure 1. 1D ^{13}C CP-MAS spectrum of the ^{13}C-labeled *Arabidopsis* primary CW, measured at 263 K on a 900 MHz NMR instrument.

for DQ excitation and reconversion, with an excitation time of 0.57 ms.

At MAS frequencies of 8−10 kHz on the 600 MHz NMR instrument, the dominant C2, C3, and C5 signals of glucose in the 70−76 ppm region give rise to spinning sidebands that overlap with the protein side chain signals. To suppress the sidebands in both dimensions of the 2D spectra without using much higher MAS frequencies, which slow spin diffusion, we implemented a triple-TOSS version of the 2D PDSD experiment using the scheme of Geen and Bodenhausen,[20] in which the TOSS sequence and its time-reversal counterpart were applied before and after the t_1 evolution period to create purely isotropic chemical shift evolution, and a third TOSS sequence was applied before the t_2 period to give isotropic chemical shifts in the ω_2 dimension. The sample was spun at 9.5 kHz for this TOSS−PDSD experiment.

To enhance the spectral resolution, we also measured 2D spectra on a 900 MHz NMR instrument at the MIT/Harvard Center for Magnetic Resonance using a 2.5 mm MAS probe. The intact wild-type CW sample was spun at 13.5 kHz and 263 K. A 2D RFDR experiment with a total mixing time of 2.37 ms, which corresponded to 32 rotor periods of π pulses,[21] was conducted to measure short-range correlation peaks. A 30 ms PDSD spectrum and a 700 ms PDSD spectrum were measured to detect longer-range correlations. Typical radiofrequency field strengths were 100−125 kHz for ^1H decoupling and 62.5 kHz for ^{13}C pulses.

To obtain spin diffusion buildup time constants, we extracted one-dimensional (1D) cross sections from the ω_2 dimension of the 2D PDSD spectra. The height $H(\omega_a,\omega_b)$ of each cross-peak at $(\omega_1 = \omega_a, \omega_2 = \omega_b)$ was divided by the integrated intensities $I(\omega_a)$ of the $\omega_1 = \omega_a$ row. For most cross sections, the integrated intensities were relatively constant with time, indicating that ^{13}C T_1 relaxation was minimal within 1.5 s. The $H(\omega_a,\omega_b)/I(\omega_a)$ values of all cross-peaks were scaled by a common factor (106.5) to normalize the maximal intensity of the iC4−iC6 cross-peak to 1. The mixing time-dependent intensities were fit to several exponential functions. For cross-peaks exhibiting only growing intensities, the fit equations were either single-exponential $(y = a - ae^{-t/\tau_c})$ or double exponential $(y = a - be^{-t/\tau_{c,1}} - ce^{-t/\tau_{c,2}})$, where a, b, and c describe the amplitudes of the buildup curves and τ_c values are the buildup time constants. For intramolecular cross-peaks whose intensities initially grew and then decayed, the fit equation was $y = (a - ae^{-t/\tau_{c,1}})[b + (1 - b)e^{-t/\tau_{c,2}}]$.

RESULTS

Polysaccharide Signals in the 2D ^{13}C−^{13}C Correlation Spectra. The CW of dark-grown *A. thaliana* has a polysaccharide composition similar to that of the CW of light-grown plants, based on the ^{13}C spectral intensities between 60 and 110 ppm of the two samples (Figure S1 of the Supporting Information). The main difference is that the light-grown plants have a higher protein content. Small differences in the relative amount of pectin and cellulose can also be discerned, with the dark-grown plants having lower pectin content (e.g., lower 99 ppm peak) and higher cellulose content (e.g., higher 89 ppm peak) than the light-grown seedlings. These minor composition differences are due to differences in the tissue types of the two plant samples. In the dark, hypocotyls are more elongated and leaf development is delayed, while in the light, hypocotyls are short and primary leaves are larger. Both hypocotyls and leaves have predominantly primary CW in their tissues.

High-resolution ^{13}C spectra of the ^{13}C-labeled primary CW were measured on the 900 MHz NMR instrument. Figure 1 shows the 1D ^{13}C spectrum, where the characteristic ^{13}C chemical shift ranges and a few relatively resolved peaks are indicated. The latter include the 89 ppm C4 signal of interior crystalline cellulose, the 65 ppm C6 signal of interior cellulose, the 84 ppm C4 signal of surface cellulose, the XG backbone, and arabinose. The methyl ^{13}C signals of the methyl ester of HGA and the acetyl group of RG I were observed at 53.5 and 21 ppm, respectively. Assignment of these two signals is based on the connectivity patterns in the 2D spectra (Figure 2).[22] The 1D ^{13}C spectrum verifies that the 2-week-old primary CW contains negligible lignin, because there is no distinct signal at 56 ppm (dashed line) for the characteristic OCH_3 moiety prevalent in lignins.[23] The low-intensity peaks at 157 and 130 ppm can be assigned to mostly tyrosine (Tyr), which serves as cross-links in several CW structural proteins.[8] The resolution of the ^{13}C spectrum can be assessed by a representative deconvolution analysis of the C1 signals at 105 and 101 ppm (Figure S2 of the Supporting Information): the 105 ppm peak contributes at most 10% of the intensity at 101 ppm, indicating good resolution of the two peaks.

dx.doi.org/10.1021/bi3015532 | *Biochemistry* 2012, 51, 9846−9856

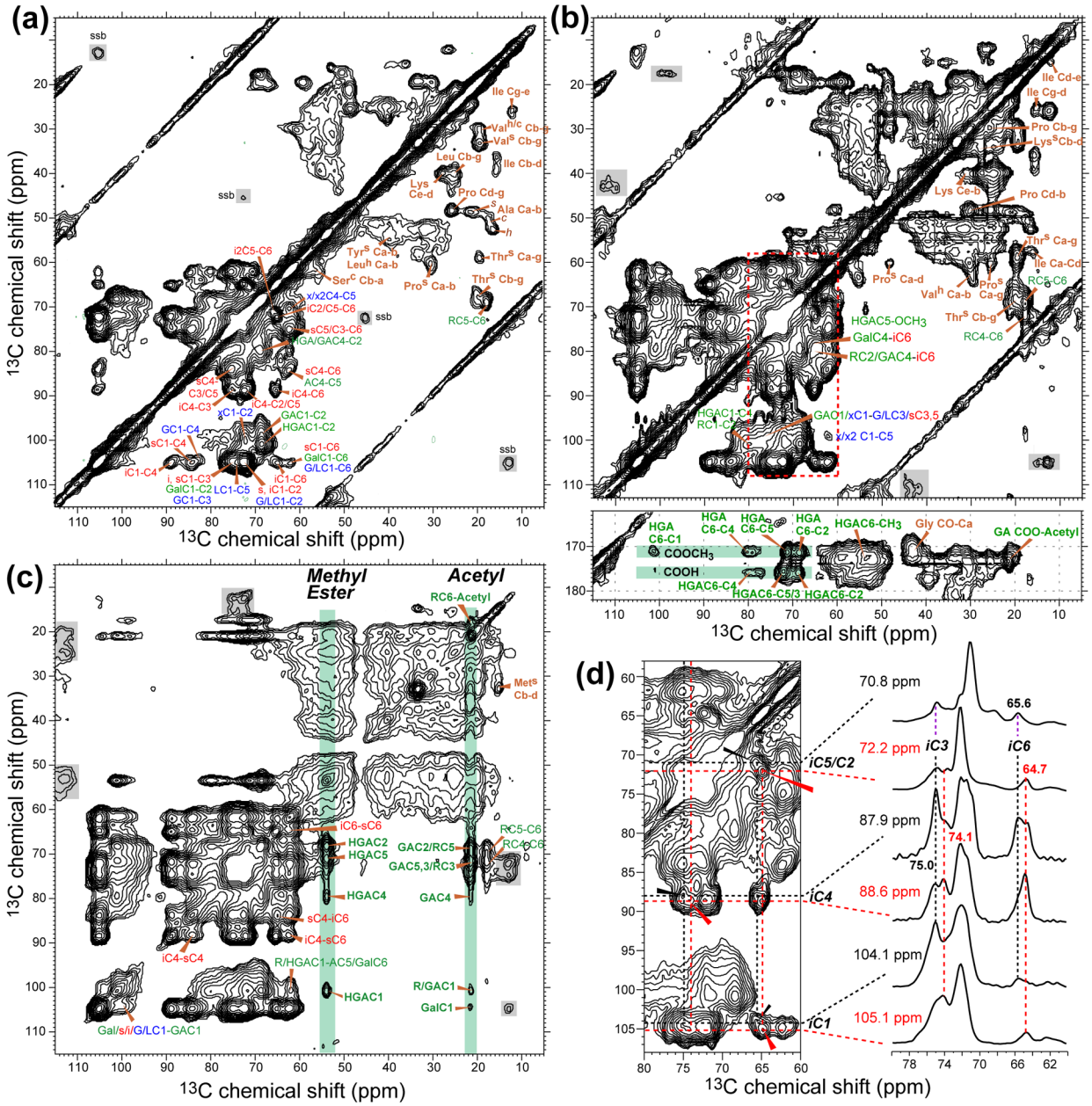

Figure 2. 2D ^{13}C correlation spectra of the ^{13}C-labeled *Arabidopsis* primary CW. (a) 2D RFDR spectrum. Cross-peaks are labeled in red for cellulose, blue for hemicellulose, green for pectins, and brown for proteins. Shaded areas denote spinning sidebands (ssb). Superscripts for amino acid assignments indicate secondary structures (s, sheet; h, helix; c, coil). (b) A 30 ms PDSD spectrum exhibiting multibond intramolecular cross-peaks. The methyl ester and acetyl cross-peaks in the 170−180 ppm region are shown below the carbohydrate and protein regions. (c) The 700 ms PDSD spectrum. (d) Expanded view of the red dashed line region of panel b and selected cross sections, which resolve two sets of interior cellulose peaks with 0.5−1.0 ppm chemical shift differences (Table S1 of the Supporting Information).

To detect cellulose−pectin contacts in the primary CW, we measured a series of 2D ^{13}C spectra with mixing times ranging from 5 ms to 1.5 s. To preferentially detect one- or two-bond cross-peaks, we measured a 2D RFDR spectrum, in which the short mixing time for active $^{13}C-^{13}C$ dipolar recoupling[21] restricts the distance upper limit. Figure 2 shows representative 2D spectra obtained with the 900 MHz NMR instrument. The RFDR spectrum is dominated by characteristic one- and two-bond cross-peaks such as C4−C3 and C4−C6 cross-peaks of the surface cellulose (s) in the 85 ppm cross section and of interior cellulose (i) in the 89 ppm cross section. In the 105 ppm cross section, strong cellulose C1−C2 and C1−C3 cross-peaks were observed. In keeping with our previous notation,[15] we use red to indicate cellulose assignment, blue for hemicellulose peaks, and green for pectin peaks. Figure 2b shows the 30 ms PDSD spectrum. Compared to those of the RFDR spectrum, the relative intensities of pectin and hemicellulose peaks increased. For example, strong intensities at ω_1 and ω_2 chemical shifts of 62 and 100 ppm, due to Xyl C6−C1 correlation are detected, and intensities at 100 and 80 ppm, due to the GalA C1−C4 peak are much stronger than in the RFDR spectrum. In the 65 ppm cross section of iC6, weak cross-peaks with the C1 carbon of Rha, GalA, and Gal appear at 101 ppm.

At 900 MHz, we resolved two types of crystalline cellulose whose ^{13}C chemical shifts differ by 0.5−1.0 ppm (Figure 2D

dx.doi.org/10.1021/bi3015532 | *Biochemistry* 2012, 51, 9846−9856

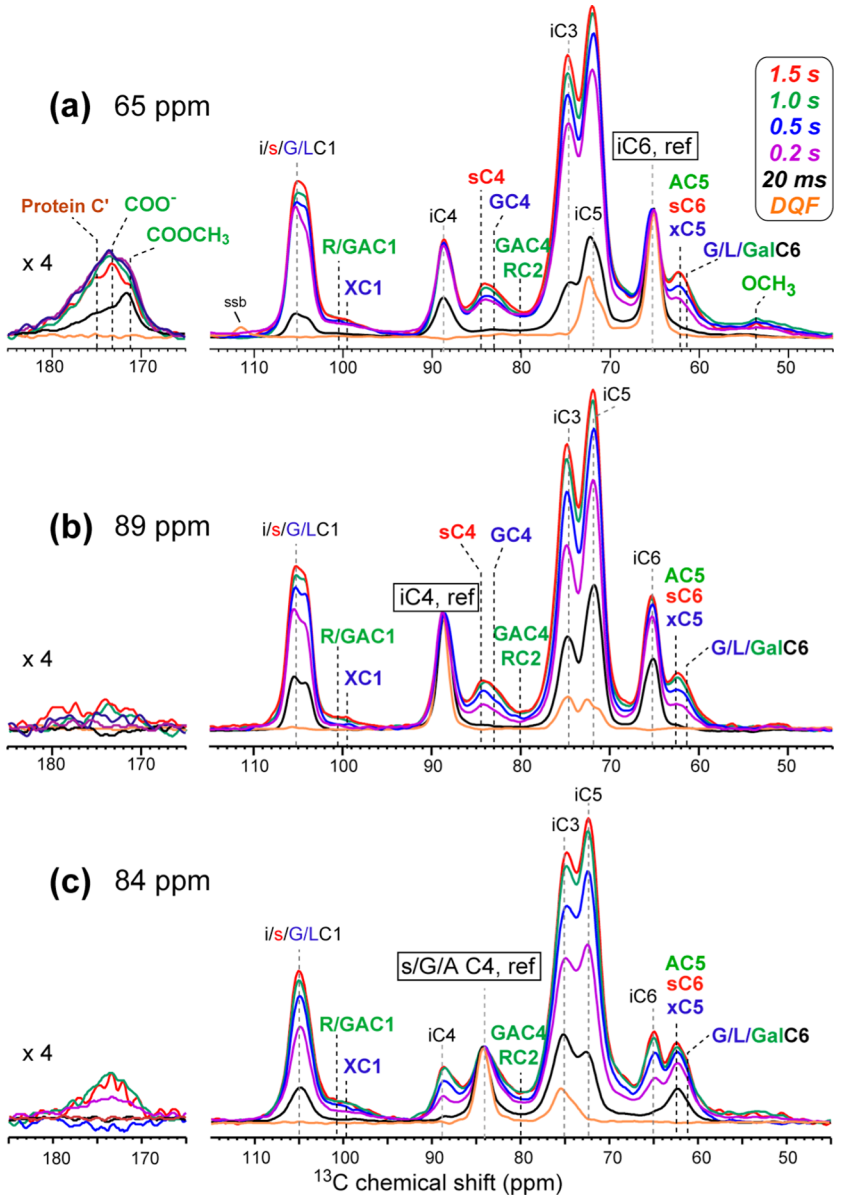

Figure 3. ω_2 cross sections of predominantly cellulose peaks from 2D PDSD and DQ filtered (DQF) spectra. (a) The 65 ppm peak of interior cellulose C6. (b) The 89 ppm peak of interior cellulose C4. (c) The 84 ppm signal of surface cellulose, XG Glc, and Ara C4. Each cross section is normalized with respect to the diagonal peak, which is boxed. Intermolecular cross-peaks are assigned in bold. The carbonyl intensities are amplified 4-fold for the sake of clarity.

and Table S1 of the Supporting Information). The C4 chemical shifts are 88.6 and 87.9 ppm, and the corresponding C6 chemical shifts are 65.6 and 64.7 ppm, respectively. Cellulose C4 and C6 chemical shifts are sensitive to the hydroxymethyl conformation and intramolecular and intermolecular H-bonding of the glucan chains.[14,24−27] For example, amorphous cellulose on the microfibril surface exhibits C4 and C6 chemical shifts of 84.5 and 62.5 ppm, respectively, which are 5 and 3 ppm smaller, respectively, than those of interior cellulose. Therefore, we tentatively attribute cellulose with the 87.9 ppm chemical shift to less ordered glucan chains.

At a longer mixing time of 700 ms, many new cross-peaks arise in the 2D spectrum (Figure 2c). The most prominent additional peaks appear in the 53.5 and 21.0 ppm cross sections and result from the methyl ester of HGA and acetyl of RG I, respectively. This assignment is based on the expected chemical shifts of these functional groups, the cross-peak patterns in the 2D spectra, and literature data of purified RG I.[22] The 53.5 ppm peak displays cross-peaks with all other carbons of HGA, while the 21 ppm peak exhibits cross-peaks with the other GalA and Rha carbons in RG I. The 21 ppm methyl carbon also shows the expected one-bond cross-peak with the 173 ppm CO signal in the 30 ms spectrum (Figure 2b), while the 53.5 ppm peak has a two-bond cross-peak with the COO group of HGA. The absence of long-range cross-peaks between these methyl carbons and other GalA carbons at shorter mixing times indicates that the separation by oxygens and the methyl dynamics present a significant spin diffusion barrier.

In addition to intramolecular pectin−pectin cross-peaks, we also observed intermolecular cross-peaks that can be assigned mostly to interior cellulose−surface cellulose contacts at long mixing times. For example, an (89, 84) ppm cross-peak is observed that can be assigned to iC4-s/G/AC4 correlation, while a (89, 62) ppm peak can be assigned to iC4 correlation

dx.doi.org/10.1021/bi3015532 | Biochemistry 2012, 51, 9846−9856

with s/G/GalC6 or A/x C5. While multiple polysaccharides can resonate at 84 and 62 ppm, the strongest contribution likely comes from the surface cellulose, because of the known tight packing of the glucan chains in the cellulose microfibril. A (99, 105) ppm cross-peak is also observed that was absent at short mixing times. This peak must be assigned to long-range correlations between the C1 atoms of GalA and Xyl and the C1 atoms of several other polysaccharides, including cellulose, the XG backbone, and Gal in RG I.

CW Protein Signals in 2D ^{13}C Correlation Spectra. The 10−60 ppm region of the ^{13}C spectra shows multiple protein cross-peaks (Figure 2a,b). We assigned the most characteristic and resolved peaks to the amino acid types based on the known compositions of CW structural proteins (Table S2 of the Supporting Information). Multiple Pro cross-peaks (Cα−Cβ and Cδ−Cγ) and a clear Lys side chain Cε−Cδ peak were observed, both of which can be attributed to PRPs. The (61, 57) ppm peak can be unambiguously assigned to Ser with coil-like conformation, which most likely results from the Ser-(Hyp)$_4$ repeat motif in HRGPs. A Hyp Cγ−Cδ cross-peak at (72.5, 58.6) ppm was observed in a DQ filtered 2D spectrum (Figure S3 of the Supporting Information). Well-resolved Ala Cα−Cβ cross-peaks in all three canonical conformations, helix, sheet, and coil, were observed, suggesting that the main Ala-containing structural protein, AGP, has diverse secondary structure. Thr, which is present in AGPs, shows two resolved cross-peaks at β-sheet chemical shifts. The aromatic region of the 2D spectra (Figure S4 of the Supporting Information) shows cross-peaks of Tyr, which serves as a cross-link in CW proteins.[8] The 130 ppm cross section of Tyr and Phe has correlations with only protein aliphatic and carbonyl signals but no correlations with polysaccharide signals, confirming that these aromatic signals result from structural proteins rather than lignins. Together, these assignments identify the main amino acid residue types in structural proteins and indicate the presence of a significant amount of β-sheet and random coil conformations.

Cross-peak Intensity Buildup with Time. To investigate cellulose−pectin interactions more quantitatively, we analyzed ω_2 cross sections of the 2D PDSD spectra as a function of mixing time. Only spectra measured on the 600 MHz NMR instrument at 253 K were used. The cross sections from the DQ filtered spectrum were superimposed for comparison, but their intensities were not included in the buildup analysis. Figure 3 shows ω_2 cross sections for three exclusively or predominantly cellulose peaks: iC6 at 65 ppm, iC4 at 89 ppm, and the 84 ppm peak due to C4 of surface cellulose, XG backbone, and Ara. To facilitate visualization of cross-peak growth with time, we scaled the cross sections such that the diagonal intensity is the same at all mixing times. Three distinct buildup behaviors were observed. The intensities of the intramolecular cross-peaks of interior cellulose built up quickly with time. For example, the 89 ppm peak in the 65 ppm cross section due to iC6−iC4 correlation reached ~40% of the maximal intensity by 20 ms, and by 200 ms, the intensity was indistinguishable from those at longer mixing times. The second buildup behavior was exemplified by interior cellulose−surface cellulose correlations. These cross-peaks were weak (~10%) at 20 ms but developed significantly (>60% of the equilibrium intensity) by 200 ms. Examples are the 85 ppm peak of s/G/A C4 in the 65 ppm cross section and the 89 ppm cross section. The third class of cross-peaks was observed between cellulose and matrix polysaccharides. For example, the 65 ppm cross section of iC6 showed weak cross-peaks with the 53.5 ppm peak of the methyl ester and the 99−101 ppm C1 signals of RG I, HGA, and XG. iC6 also displayed cross-peaks with the CO group of HGA, RG I, and proteins between 170 and 180 ppm. Cross-peak intensities at 80 ppm were also detected, which must be assigned to pectins, specifically a combination of GalA C4 and Rha C2 in RG I.[15] These intermolecular cross-peaks became significant by ~200 ms in the iC6 cross section but required more time to develop for iC4, with weaker final intensities (Figure 3b). The slower spin diffusion from iC4 is reasonable, because the buried position of C4 in the glycosidic linkage of glucan chains should prevent close contacts with other polysaccharides compared to C6, which lies on the periphery of the glucan chains. Interior cellulose C4 did not develop cross-peaks with the methyl ester and carboxyl carbons of GalA by 1.5 s, which may be partly attributed to the lower spin diffusion efficiency between carbons with large chemical shift differences. Compared to iC4, the 84 ppm mixed C4 signal of surface cellulose, the XG backbone, and Ara (Figure 3c) has significantly higher cross-peaks with pectin signals at 173, 101, and 80 ppm, indicating that surface cellulose and hemicelluloses are closer to pectins than interior cellulose.

Figure 4 shows the 1D cross sections at pectin and hemicellulose chemical shifts of 101, 99, and 80 ppm. The

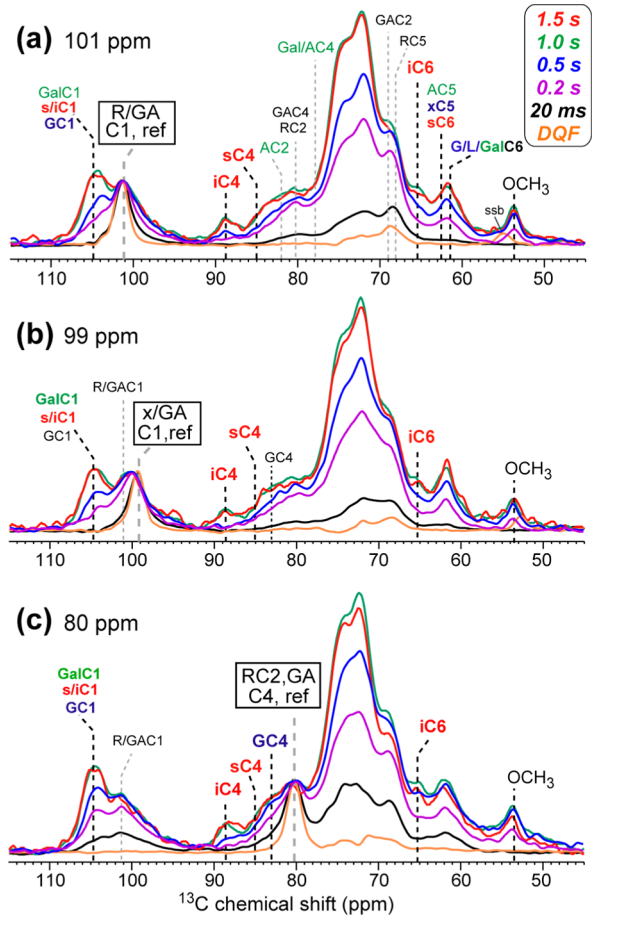

Figure 4. ω_2 cross sections of pectin peaks from 2D ^{13}C spectra. (a) The 101 ppm cross section of Rha and GalA C1. (b) The 99 ppm cross section of Xyl and GalA C1. (c) The 80 ppm cross section of GalA C4 and Rha C2. Note the strong methyl ester cross-peak at 53.5 ppm.

dx.doi.org/10.1021/bi3015532 | Biochemistry 2012, 51, 9846−9856

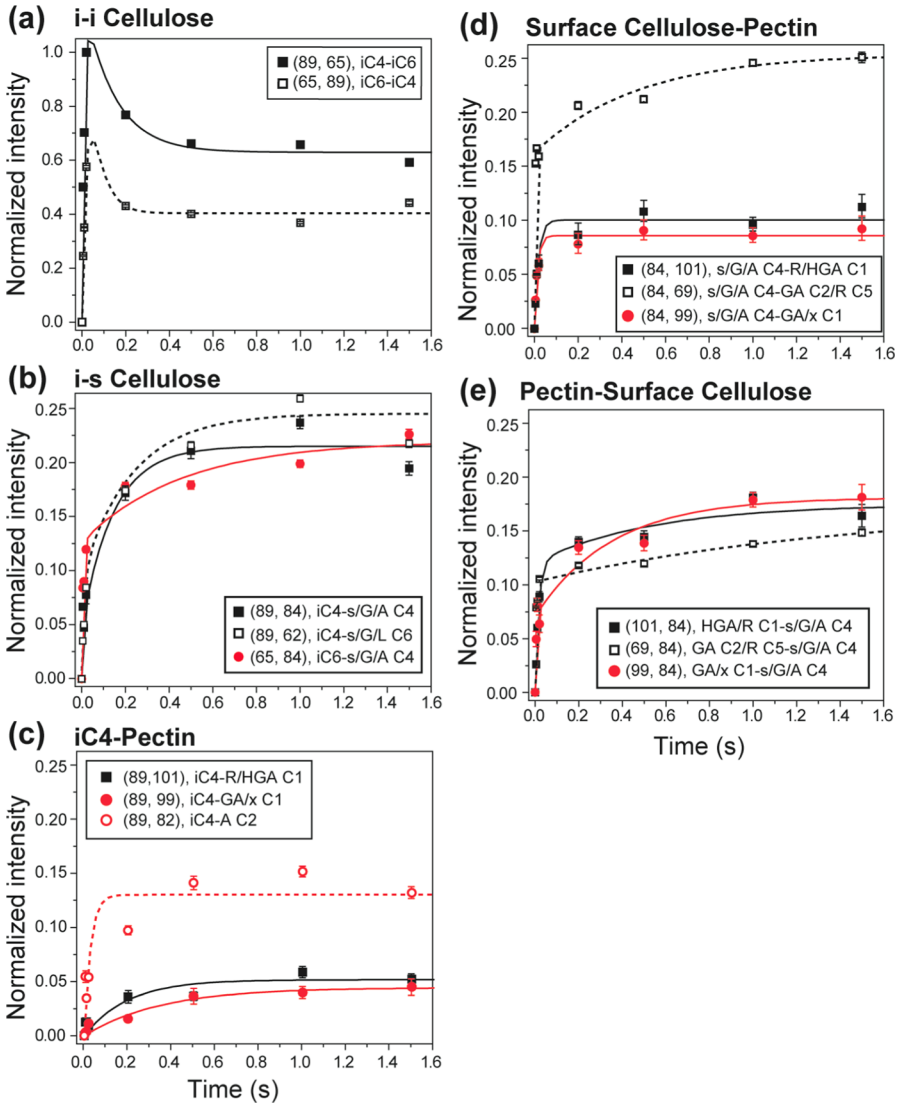

Figure 5. Buildup curves of representative cross-peaks from 2D PDSD spectra. (a) Intramolecular cross-peaks within interior cellulose. (b) Intermolecular surface cellulose−interior cellulose peaks. (c) iC4−pectin cross-peaks. (d) Surface cellulose−pectin cross-peaks. (e) Pectin−surface cellulose cross-peaks. The (ω_1,ω_2) chemical shifts (parts per million) and peak assignments are indicated.

101 ppm peak results from HGA and Rha C1; the 80 ppm peak is due to GA C4 and Rha C2, and the 99 ppm peak is assigned to GA and Xyl C1. These cross sections show significant intensities at 65 ppm (iC6) and 89 ppm (iC4), further verifying cellulose−pectin contact. The growth of the 105 ppm peak is clearly slower than that of the diagonal 101 ppm peak in the 101 ppm cross section, confirming the resolvability of these two peaks. Similarly, the 80 ppm signal of Rha C2 and GA C4 is resolved from the 83−85 ppm peaks of Glc C4 in XG and surface cellulose (Figure 4c). All three cross sections show much higher methyl ester peaks (53.5 ppm) than in the cellulose cross sections, consistent with the partial intramolecular (pectin−pectin) nature of these cross-peaks.

More quantitative information about the spatial proximity among the polysaccharides is obtained by analyzing the cross-peak intensities as a function of mixing time (Figure 5). The buildup time constants reflect the average $^{13}C-^{13}C$ distances. At 253 K, cellulose and pectins have similar C−H order parameters of 0.88 (Figure S5 of the Supporting Information), indicating similar spin diffusion efficiencies for all polysaccharides. We compared the buildup curves of different categories of cross-peaks. Intramolecular spin diffusion within interior cellulose is expected to be fast, while cross-peaks between interior and surface cellulose give a benchmark of the intermolecular spin diffusion rates between two polysaccharides with known structure and packing. With these two references, we analyzed the cellulose−pectin cross-peak buildup rates. The well-resolved cross-peaks between interior cellulose C4 and C6 exhibit a fast initial buildup followed by a slow decay (Figure 5a). The initial rise time constant is 10−30 ms (Table S3 of the Supporting Information), which reflects the two-bond magnetization transfer rate, whereas the slow decay reflects the loss of magnetization to other polysaccharides. We normalized all cross-peak intensities by the integrated intensity of each cross section. Because the integrated intensities at $\omega_1 = \omega_a$ and $\omega_1 = \omega_b$ can differ due to different CP efficiencies or partial resonance overlap at one of the two positions, the pair of symmetric cross-peaks at (ω_a,ω_b) and (ω_b,ω_a) can have different normalized intensities. However, the buildup rates were the same within experimental uncertainty. For example, the (89, 65) ppm cross-peak has 1.6-fold higher intensities than the (65, 89) ppm peak due to the higher intensity of the iC6

dx.doi.org/10.1021/bi3015532 | *Biochemistry* 2012, 51, 9846−9856

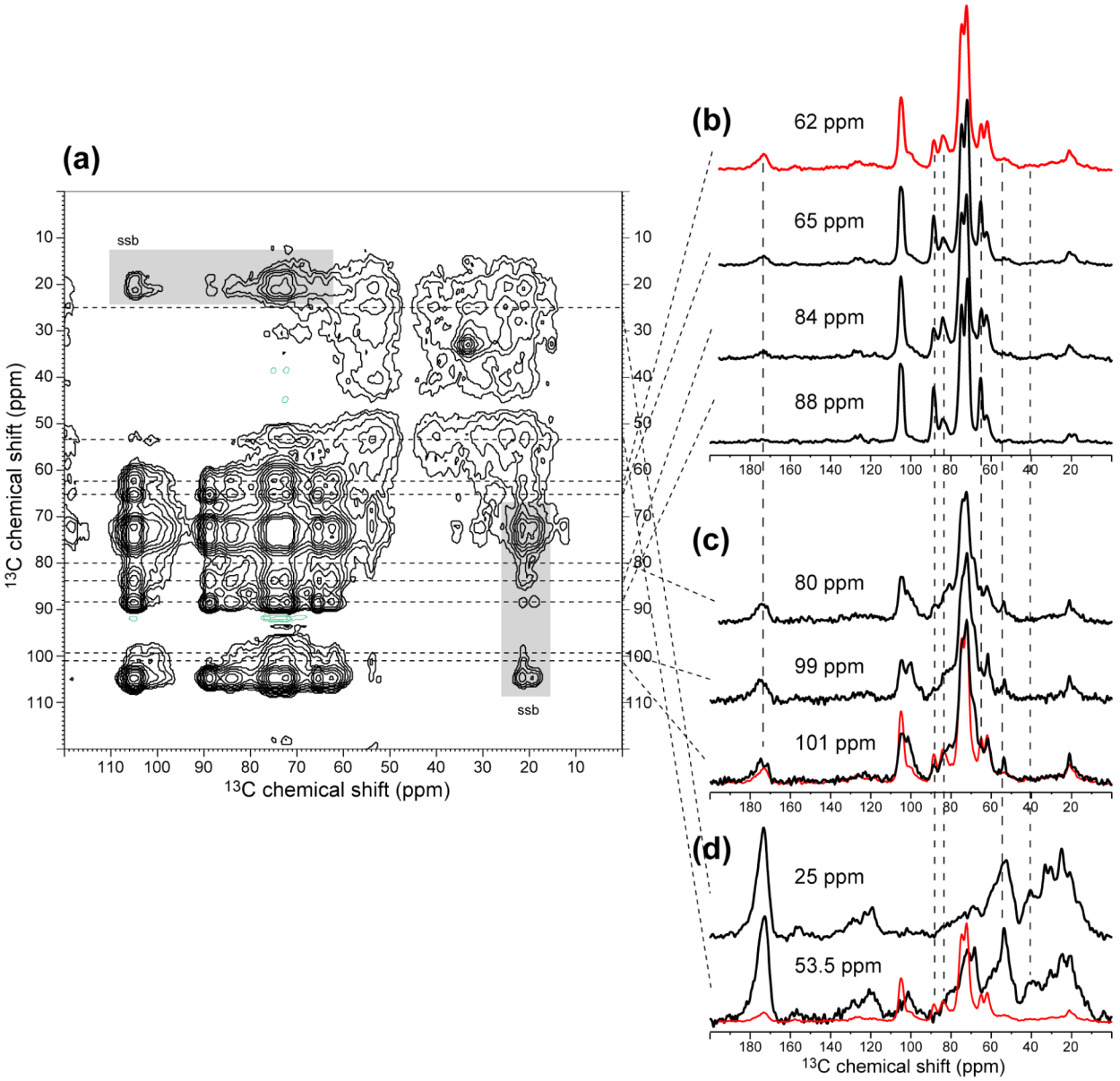

Figure 6. Lack of complete equilibration of ^{13}C magnetization by 1.5 s. (a) 2D ^{13}C PDSD spectrum at 1.5 s mixing. Shaded areas denote spinning sidebands. (b) Cross sections of predominantly cellulose peaks, including iC6 (65 ppm), iC4 (88 ppm), s/G/A C4 (84 ppm), and s/G/Gal C6 and A/x C5 (62 ppm). (c) Cross sections of pectin peaks, including the 80 ppm peak of GalA C4 and Rha C2, the 99 ppm peak of Xyl C1 and GalA C1, and the 101 ppm peak of Rha and HGA C1. (d) Selected protein cross sections. The 53.5 ppm cross section has contributions from both the methyl ester and proteins. The 62 ppm cross section (red) is overlaid in panels c and d to guide the eye for differences in the intensity patterns.

peak (i.e., larger denominator), but the buildup rates are the same between the two peaks. Most importantly, the "overshoot" of buildup intensities is a distinct signature of short-distance transfer for spins in close proximity of each other.

In comparison, all intermolecular cross-peaks exhibit only intensity growth and no decay. The surface cellulose−interior cellulose buildup curves (Figure 5b) show time constants of 150−450 ms (Table S3 of the Supporting Information), reflecting spin diffusion rates between glucan chains packed within a diameter of 3−5 nm. We also detected a component of fast initial rise with time constants of ≤10 ms, which we attribute to the closest approach between two neighboring glucan chains.

The cellulose−pectin buildup curves show important similarities to the cellulose spin diffusion curves. First, surface cellulose exhibits a fast initial buildup to pectin (Figure 5d,e), similar to the surface cellulose−interior cellulose spin diffusion. Interior cellulose does not have this initial component (Figure 5c), consistent with the larger separation of interior cellulose from the matrix polysaccharides. Second, the slow component of cellulose−pectin buildup curves has time constants of 200−550 ms, similar to those of surface cullulose−interior cellulose buildup curves, indicating that cellulose−pectin separations are overall comparable to the surface cellulose−interior cellulose separation. However, the pectin−cellulose magnetization transfer equilibrates at lower intensities, indicating that only a fraction of cellulose chains is in contact with pectins. For example, the intensities of the 89 ppm cross-peaks with 99, 101, and 82 ppm are 25−50% of the iC4−surface cellulose cross-peak intensities, indicating that only 25−50% of interior cellulose chains are in close contact with pectins. Thus, the intensities and buildup rates contain independent information

dx.doi.org/10.1021/bi3015532 | *Biochemistry* 2012, 51, 9846−9856

about the spatial proximity of pectin and cellulose. Comparison of surface cellulose−pectin peaks and surface cellulose−interior cellulose cross-peaks confirms that the fraction of surface cellulose in contact with pectins is ∼50% of the fraction of surface cellulose that interacts with interior cellulose.

The intrinsically distributed nature of the intermolecular distances and the involvement of relayed through-bond magnetization transfer in the uniformly ^{13}C-labeled plant CW make it difficult to derive precise distances from these buildup curves, but the average buildup time constants of each category of cross-peaks give a semiquantitative estimate of the relative intermolecular separations. Between surface and interior cellulose, the average buildup time constant for the long-time component is 240 ms (Table S3 of the Supporting Information), while the average long-time constant of cellulose−pectin cross-peaks is 410 ms. Therefore, the average cellulose−pectin separation is only modestly longer than the average surface cellulose−interior cellulose separation, and pectin remains well within ^{13}C spin diffusion reach of the cellulose microfibril. Taken together, these data indicate that a significant fraction of pectins comes into molecular contact (<6 Å) with cellulose.

At sufficiently long ^{13}C spin diffusion mixing times, all molecules in a molecularly homogeneous mixture should equilibrate their magnetization, so that every cross section of a 2D spectrum should exhibit the same intensity profile (Figure S6 of the Supporting Information). Figure 6 displays the 2D PDSD spectrum of the CW at a mixing time of 1.5 s. The 60−110 ppm polysaccharide region of the 2D spectrum shows extensive magnetization transfer, and the 10−60 ppm protein region of the spectrum also shows extensive cross-peaks within this region. However, few cross-peaks exist between the two regions, with the exception of the acetyl peak at 21 ppm. The polysaccharide 1D cross sections (Figure 6b,c) have similar intensity patterns, which differ from the protein cross sections (Figure 6d). These observations indicate that the proteins are relatively separated from the polysaccharides (by more than ∼1 nm). Further inspection indicates subtle intensity differences among different polysaccharides. For example, the 62 and 84 ppm cross sections, which result from a mixture of surface cellulose, XG, and pectins, differ from the interior cellulose cross sections at 65 and 88 ppm in their relative intensities of the 88 and 84 ppm peaks. Thus, even at a long mixing time of 1.5 s, the glucan chains within the cellulose microfibril have not completely equilibrated their magnetization. Similarly, although the various pectin cross sections resemble each other, they differ subtly from the cellulose cross sections, particularly at 80, 99, and 101 ppm. The 53.5 ppm cross section is a combination of the pectin intensities and the protein side chain intensities (Figure 6d). These results indicate that although pectins and cellulose contact each other at various locations of the microfibril, they are not fully mixed on the molecular level. This is reasonable, because the 3−5 nm diameter of the cellulose microfibrils presents a natural barrier to intermolecular contact with matrix polysaccharides, so that the glucan chains within the microfibrils should still be dominated by glucan−glucan contacts. The more surprising finding of these 2D spectra is that most CW proteins appear to be outside molecular contact of most polysaccharides. They may be located in the 20−40 nm spacing between cellulose microfibrils[28−30] and form a distinct domain.

DISCUSSION

Elucidating the 3D architecture of the polysaccharides and proteins in plant cell walls requires high-resolution solid-state NMR spectra. Here we enhanced spectral resolution by using higher magnetic fields and by measuring multiple 2D spectra as a function of mixing time. The latter allows the identification of intermolecular cross-peaks as those signals that appear at long mixing times but absent at short times. As a result, the information content of multiple 2D spectra can be comparable to or even higher than that of a single 3D spectrum. Distinct spin diffusion buildup behaviors were observed, indicating that cellulose and pectin peaks are sufficiently resolved. ^{13}C spin diffusion is sensitive to internuclear distances up to ∼6 Å; thus, the buildup curve analysis reveals information about subnanometer spatial proximities.

Analyses of the 2D ^{13}C correlation spectra provided semiquantitative support for the finding[15,31] that all three major polysaccharides of the primary CW, cellulose, hemicellulose, and pectins, are in molecular contact with each other (Figure 7). The main distinction is the fraction of a particular

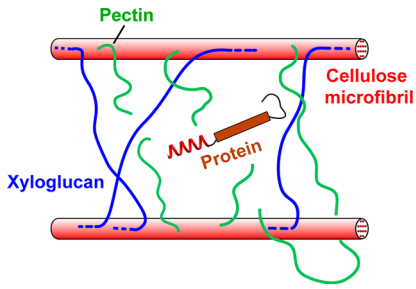

Figure 7. Model of the primary plant cell wall architecture determined from 2D ^{13}C NMR spectra. Some pectin segments are in the proximity of cellulose microfibrils, and a small fraction of XG is entrapped in the cellulose microfibrils. All three major polysaccharides form a single cohesive network in the primary cell wall. The structural proteins are relatively separated from the polysaccharides and are rich in β-sheet and coil conformations.

polysaccharide exhibiting close contact with another polysaccharide, as manifested by the equilibrium magnetization at long mixing times. The presence of close cellulose−pectin proximity is unambiguously indicated by cross-peaks from cellulose (e.g., 65, 89, and 84 ppm) to exclusively pectin signals (Figure 3). The time constants of pectin−cellulose cross-peak buildup are 200−540 ms, which are comparable to the time constants for surface cellulose−interior cellulose cross-peaks. The cellulose−pectin peaks equilibrate at lower intensities than the interior cellulose−surface cellulose cross-peaks, indicating that 25−50% of the cellulose chains are in close contact with pectins.

Biochemical evidence of cellulose−pectin proximity has been reported. For example, it was shown that sugar beet and potato pectins, which are rich in neutral sugar side chains such as arabinans and galactans, can absorb to cellulose in vitro, suggesting hydrogen bond formation.[32] Debranched arabinan showed higher binding affinity than branched arabinan, similar to the binding of XG to cellulose. When the sugar beet and potato cell walls were treated with high concentrations of alkali, the remaining residues were found to contain Ara, GalA, and Glc, suggesting that the major polysaccharides in these residues are arabinan-rich pectins and cellulose.[32] The current SSNMR data are consistent with these observations and provide direct

dx.doi.org/10.1021/bi3015532 | *Biochemistry* 2012, 51, 9846−9856

evidence of pectin−cellulose proximity in an intact CW. The numerous RG I−cellulose and HGA−cellulose interactions are consistent with the absence of extensive coating of the microfibril surface by hemicellulose, which was deduced from the lack of abundant cross-peaks between XG and cellulose.[15] On the other hand, the pectin−cellulose contacts do not mean that these two polysaccharides are homogeneously mixed on the molecular level, because the ^{13}C magnetization of the two polysaccharides is not fully equilibrated by 1.5 s. This nanoscale heterogeneity is entirely reasonable given the 3−5 nm diameter of the cellulose microfibrils and is consistent with the previously observed dynamic differences between cellulose and pectins at ambient temperature.[15,31]

In contrast to the proximity among the polysaccharides, the structural proteins in the primary CW appear to be separated from the polysaccharides by more than a nanometer (Figure 7), as evidenced by the conspicuous lack of protein−polysaccharide cross-peaks. Among the cell wall proteins, AGPs are carbohydrate-rich (∼90%) proteins that may be expected to show significant polysaccharide−protein cross-peaks. The fact that such peaks are absent in our spectra may be due to the fact that the protein component in AGPs accounts for a very small fraction (∼10%), so that the probability of protein−polysaccharide spatial contact is statistically low. Moreover, structural proteins typically are present at low levels in hypocotyls and tissues of young seedlings;[33] thus, they are present at low concentrations in our CW samples. Glycoproteins have been proposed to be important in early wall formation. For example, *Arabidopsis* with a mutation in HRGP was shown to be embryo-lethal, most likely because of the failure in cell plate formation,[9] and O-glycosylation of HRGP is crucial for root hair wall assembly.[34] However, how the backbone conformation and intermolecular interactions of structural proteins underlie wall formation is not yet understood. Recently, biomechanical properties of cell walls in wild-type and XG-deficient mutant plants were studied, and significant contributions of pectins and arabinoxylan to the CW mechanics were demonstrated.[29] However, the authors did not detect a similar contribution of the wall proteins to wall mechanics, suggesting that while pectins and hemicelluloses share load-bearing functions with cellulose, CW proteins might not be involved in this load-bearing network. Further studies are necessary to elucidate the structure−function relationship of the structural proteins in the cell wall.

CONCLUSION

These 2D ^{13}C spin diffusion NMR spectra indicate unambiguously that direct cellulose−pectin spatial contacts exist in the *Arabidopsis* primary cell wall. On the basis of the spin diffusion buildup time constants, the minimal distances between cellulose and pectins are comparable to the separation between interior and surface cellulose chains, but only 25−50% of the cellulose chains exhibit such close contacts with pectins. In contrast, the structural proteins are separated by more than a nanometer from the polysaccharides, resulting in a lack of protein−polysaccharide cross-peaks at long mixing times. These results indicate that load bearing in the primary cell wall is accomplished by a single network of all three major polysaccharides, supporting a revision of the traditional cell wall structural model.

ASSOCIATED CONTENT

Supporting Information

Tables and additional NMR spectra. This material is available free of charge via the Internet at http://pubs.acs.org.

AUTHOR INFORMATION

Corresponding Author

*Telephone: (515) 294-3521. Fax: (515) 294-0105. E-mail: mhong@iastate.edu.

Funding

This work was supported by the U.S. Department of Energy, Office of Basic Energy Sciences, Division of Materials Sciences and Engineering, via Grant AL-90-360-001.

Notes

The authors declare no competing financial interest.

ACKNOWLEDGMENTS

We thank Professor Daniel Cosgrove for insightful discussions. The 900 MHz NMR spectra were measured at the MIT/Harvard Center for Magnetic Resonance, supported by National Institutes of Health Grant P41-EB-002026.

REFERENCES

(1) Carpita, N. C., and McCann, M. (2000) The cell wall. In *Biochemistry and Molecular Biology of Plants* (Buchanan, B. B., Gruissem, W., and Jones, R. L., Eds.) American Society of Plant Physiologists, Rockville, MD.

(2) Carpita, N. C., and Gibeaut, D. M. (1993) Structural models of primary cell walls in flowering plants: Consistency of molecular structure with the physical properties of the walls during growth. *Plant J. 3*, 1−30.

(3) Sarkar, P., Bosneaga, E., and Auer, M. (2009) Plant cell walls throughout evolution: Towards a molecular understanding of their design principles. *J. Exp. Bot. 60*, 15−35.

(4) Albersheim, P., Darvill, A., Roberts, K., Sederoff, R., and Staehelin, A. (2010) *Plant Cell Walls*, Garland Science, Taylor & Francis Group, LLC, New York.

(5) Kennedy, C. J., Cameron, G. J., Sturcova, A., Apperley, D. C., Altaner, C., Wess, T. J., and Jarvis, M. C. (2007) Microfibril diameter in celery collenchyma cellulose: X-ray scattering and NMR evidence. *Cellulose 14*, 235−246.

(6) Buchanan, B. B., Gruissem, W., and Jones, R. L. (2000) *Biochemistry and Molecular Biology of Plants*, American Society of Plant Physiologists, Rockville, MD.

(7) Caffall, K. H., and Mohnen, D. (2009) The structure, function, and biosynthesis of plant cell wall pectic polysaccharides. *Carbohydr. Res. 344*, 1879−1900.

(8) Cegelski, L., O'Connor, R. D., Stueber, D., Singh, M., Poliks, B., and Schaefer, J. (2010) Plant cell-wall cross-links by REDOR NMR spectroscopy. *J. Am. Chem. Soc. 132*, 16052−16057.

(9) Cannon, M. C., Terneus, K., Hall, Q., Tan, L., Wang, Y., Wegenhart, B. L., Chen, L., Lamport, D. T. A., Chen, Y., and Kieliszewski, M. J. (2008) Self-assembly of the plant cell wall requires an extensin scaffold. *Proc. Natl. Acad. Sci. U.S.A. 105*, 2226−2231.

(10) Lamport, D. T. A., Kieliszewski, M. J., Chen, Y., and Cannon, M. C. (2011) Role of the extensin superfamily in primary cell wall architecture. *Plant Physiol. 156*, 11−19.

(11) Hedenström, M., Wiklund-Lindström, S., Oman, T., Lu, F., Gerber, L., Schatz, P., Sundberg, B., and Ralph, J. (2009) Identification of lignin and polysaccharide modifications in Populus wood by chemometric analysis of 2D NMR spectra from dissolved cell walls. *Mol. Plant*, 933−942.

(12) Lu, F., and Ralph, J. (2003) Non-degradative dissolution and acetylation of ball-milled plant cell walls: High-resolution solution-state NMR. *Plant J. 35*, 535−544.

(13) Jarvis, M. C. (1992) Self-assembly of plant cell walls. *Plant, Cell Environ. 15*, 1−5.
(14) Davies, L. M., Harris, P. J., and Newman, R. H. (2002) Molecular ordering of cellulose after extraction of polysaccharides from primary cell walls of *Arabidopsis thaliana*: A solid-state CP/MAS ^{13}C NMR study. *Carbohydr. Res. 337*, 587−593.
(15) Dick-Pérez, M., Zhang, Y., Hayes, J., Salazar, A., Zabotina, O. A., and Hong, M. (2011) Structure and interactions of plant cell-wall polysaccharides by two- and three-dimensional magic-angle-spinning solid-state NMR. *Biochemistry 50*, 989−1000.
(16) Harris, D. M., Corbin, K., Wang, T., Gutierrez, R., Bertolo, A. L., Petti, C., Smilgies, D. M., Estevez, J. M., Bonetta, D., Urbanowicz, B. R., Ehrhardt, D. W., Somerville, C. R., Rose, J. K., Hong, M., and Debolt, S. (2012) Cellulose microfibril crystallinity is reduced by mutating C-terminal transmembrane region residues CESA1A903V and CESA3T942I of cellulose synthase. *Proc. Natl. Acad. Sci. U.S.A. 109*, 4098−4103.
(17) Cosgrove, D. J. (2001) Wall structure and wall loosening. A look backwards and forwards. *Plant Physiol. 125*, 131−134.
(18) Cosgrove, D. J. (2005) Growth of the plant cell wall. *Nat. Rev. Mol. Cell Biol. 6*, 850−861.
(19) Hohwy, M., Jakobsen, H. J., Eden, M., Levitt, M. H., and Nielsen, N. C. (1998) Broadband dipolar recoupling in the nuclear magnetic resonance of rotating solids: A compensated C7 pulse sequence. *J. Chem. Phys. 108*, 2686−2694.
(20) Geen, H., and Bodenhausen, G. (1992) Pure absorption-mode chemical-exchange nuclear-magnetic-resonance spectroscopy with suppression of spinning side-band in a slowly rotating solids. *J. Chem. Phys. 97*, 2928−2937.
(21) Bennett, A. E., Ok, J. H., Griffin, R. G., and Vega, S. (1992) Chemical shift correlation spectroscopy in rotating solids: Radio-frequency-driven dipolar recoupling and longitudinal exchange. *J. Chem. Phys. 96*, 8624−8627.
(22) Larsen, F. H., Byg, I., Damager, I., Diaz, J., Engelsen, S. B., and Ulvskov, P. (2011) Residue specific hydration of primary cell wall potato pectin identified by solid-state ^{13}C single-pulse MAS and CP/MAS NMR spectroscopy. *Biomacromolecules 12*, 1844−1850.
(23) Ralph, J., and Landucci, L. L. (2008) NMR of Lignins. In *Lignin and Lignans: Advances in Chemistry* (Heitner, C., Dimmel, D. R., and Schmidt, J. A., Eds.) CRC Press, Taylor & Francis Group, Boca Raton, FL.
(24) Atalla, R. H., and VanderHart, D. L. (1984) Native Cellulose: A Composite of Two Distinct Crystalline Forms. *Science 223*, 283−285.
(25) Atalla, R. H., and Vanderhart, D. L. (1999) The role of solid state ^{13}C NMR spectroscopy in studies of the nature of native celluloses. *Solid State Nucl. Magn. Reson. 15*, 1−19.
(26) Newman, R. H., and Davidson, T. C. (2004) Molecular conformations at the cellulose−water interface. *Cellulose 11*, 23−32.
(27) Viëtor, R. J., Newman, R. H., Ha, M. A., Apperley, D. C., and Jarvis, M. C. (2002) Conformational features of crystal-surface cellulose from higher plants. *Plant J. 30*, 721−731.
(28) McCann, M. C., Wells, B., and Roberts, K. (1990) Direct visualization of cross-links in the primary plant cell wall. *J. Cell Sci. 96*, 323−334.
(29) Park, Y. B., and Cosgrove, D. J. (2012) Changes in cell wall biomechanical properties in the xyloglucan-deficient xxt1/xxt2 mutant of *Arabidopsis*. *Plant Physiol. 158*, 465−475.
(30) Cosgrove, D. J. (1997) Assembly and enlargement of the primary cell wall in plants. *Annu. Rev. Cell Dev. Biol. 13*, 171−201.
(31) Dick-Pérez, M., Wang, T., Salazar, A., Zabotina, O. A., and Hong, M. (2012) Multidimensional Solid-State NMR Studies of the Structure and Dynamics of Pectic Polysaccharides in Uniformly ^{13}C-Labeled *Arabidopsis* Primary Cell Walls. *Magn. Reson. Chem. 50*, 539−550.
(32) Zykwinska, A. W., Ralet, M. C., Garnier, C. D., and Thibault, J. F. (2005) Evidence for in vitro binding of pectin side chains to cellulose. *Plant Physiol. 139*, 397−407.
(33) Irshad, M., Canut, H., Borderies, G., Pont-Lezic, R., and Jamet, E. (2008) A new picture of cell wall protein dynamics in elongating cells of *Arabidopsis thaliana*: Confirmed actors and newcomers. *BMC Plant Biol. 8*, 94.
(34) Velasquez, S. M., Ricardi, M. M., Dorosz, J. G., Fernandez, P. V., Nadra, A. D., Pol-Fachin, L., Egelund, J., Gille, S., Harholt, J., Ciancia, M., Verli, H., Pauly, M., Bacic, A., Olsen, C. E., Ulvskov, P., Petersen, B. L., Somerville, C. R., Iusem, N. D., and Estevez, J. M. (2011) O-Glycosylated cell wall proteins are essential in root hair growth. *Science 332*, 1401−1403.

Supporting Information

Pectin-Cellulose Interactions in *Arabidopsis* Primary Cell Wall by Two-Dimensional Magic-Angle-Spinning Solid-State NMR

Tuo Wang, Olga Zabotina, and Mei Hong

Table S1. Two sets of interior cellulose ^{13}C chemical shifts (ppm) resolved at the 900 MHz NMR.

Cellulose	C1	C2	C3	C4	C5	C6
Interior 1	105.1	72.2	74.1	88.6	72.2	64.7
Interior 2	104.1	72.2	75.0	87.9	70.8	65.6

Table S2. ^{13}C chemical shifts (ppm) of assigned protein residues in *Arabidopsis* primary cell wall. The ^{13}C chemical shifts are referenced to neat TMS.

Residue	CO	Cα	Cβ	Cγ	Cδ	Cε	Cζ
Gly	171.9 173.3	43.5 43.5					
Hyp				72.5	58.6		
Lys			33.7		27.5	40.1	
Pro		60.0	30.7	25.7	48.2		
Ala		48.6 50.1 52.2	21.1 17.4 16.7				
Tyr		54.4	37.8 42.0	133.8	131.1	115.3	157.2/155.8 157.2
Phe		55.1	36.7	137.0	129.2	129.2	127.0
Ser		55.9	62.2				
Thr		58.8	67.5	19.7			
Ile		57.3	38.8 35.6	26.1	15.6 15.6	12.6	
Leu		55.3 51.2	40.1 41.5	25.3 24.3	 21.1		
Val			32.7 29.9	19.3 19.3			

Table S3. Spin diffusion buildup time constants of polysaccharide cross peaks in primary cell wall.

(ω_1, ω_2) (ppm)	Assignment	τ_1 (ms)	τ_2 (ms)
Interior-interior cellulose			
(89, 65)	iC4 – iC6	10±1.9	
(65, 89)	iC6 – iC4	29±45	
(89, 72)	iC4 – iC5/iC2, s/G/x/L C2, GA/R C3, Gal/GA C5	5.4 ± 1.7	
(65, 105)	iC6 – i/s/Gal/G/L C1	27±3.5	
(65, 75)	iC6 – iC3, sC3/5, Gal C2/3, GC3/5, LC5, x C3	15±1.7	
Interior-surface cellulose			
(89, 84)	iC4 – s/G/A C4	8.1±20 (24%)	150±94 (76%)
(89, 62)	iC4 – s/G/Gal C6, A/x C5	12±14 (37%)	230±130 (63%)
(65, 84)	iC6 – s/G/A C4	6.3±3.1 (58%)	460±380 (42%)
Surface-interior cellulose			
(84, 89)	s/G/A C4 – iC4	3.4±2.2 (34%)	190±53 (66%)
(84, 65)	s/G/A C4 – iC6	2.0±1.6 (27%)	150±24 (73%)
(62, 89)	s/G/A C6 – iC4	3.5±2.9 (23%)	250±50 (77%)
(84, 62)	s/G/A C4 – s/G/Gal C6, A/x C5	12±4.2	
Interior-pectin cellulose			
(89, 101)	iC4 – HGA/R C1		200±90
(89, 82)	iC4 – A C2	29±11	
(89, 99)	iC4 – GA/X C1		350±100
(89, 69)	iC4 – residual iC5, GA C2, R C5	6.7±2.6	
(65, 101)	iC6 – HGA/R C1	5.2±1.1	
(65,105)	iC6 – i/s/Gal/G/L C1	27±3.5	
(65, 69)	iC4 – GA C2, R C5		
(65, 99)	iC4 – GA/X C1	7.5±1.2	
Pectin-interior cellulose			
(99, 89)	GA/Xyl C1 – iC4		370±190
(82, 89)	A C2 – iC4	1.0±6.1 (37%)	510±170 (63%)
(101, 65)	HGA/Rha C1 – iC6	11±11 (44%)	490±550 (56%)
Surface-pectin cellulose			
(84, 101)	s/G/A C4 – HGA/R C1	18±3.5	
(84, 99)	s/G/A C4 – GA/X C1	14±2.0	
(84, 69)	s/G/A C4 – GA C2, R C5	1.8±0.70 (64%)	470± 180(36%)
Pectin-surface cellulose			
(101, 84)	HGA/R C1 – s/G/A C4	16±5.8 (69%)	540±720 (31%)
(99, 84)	GA/X C1 – s/G/A C4	3.6±2.9 (39%)	350±170 (61%)
(80, 84)	GA C4/R C2 – s/G/A C4	17±23	
Pectin-pectin			
(101, 80)	HGA/R C1 – GA C4/ R C2	13±2.6	

(101, 69)	HGA/R C1 – GA C2/ R C5	4.0±0.7	
(80, 101)	GA C4/ R C2 – HGA/R C1	14±1.7	
(69, 101)	GA C2/ R C5 – HGA/R C1	4.0±0.6	
(101, 54)	HGA/R C1– OCH_3		160±40
(54, 101)	OCH_3 – HGA/R C1		160±25

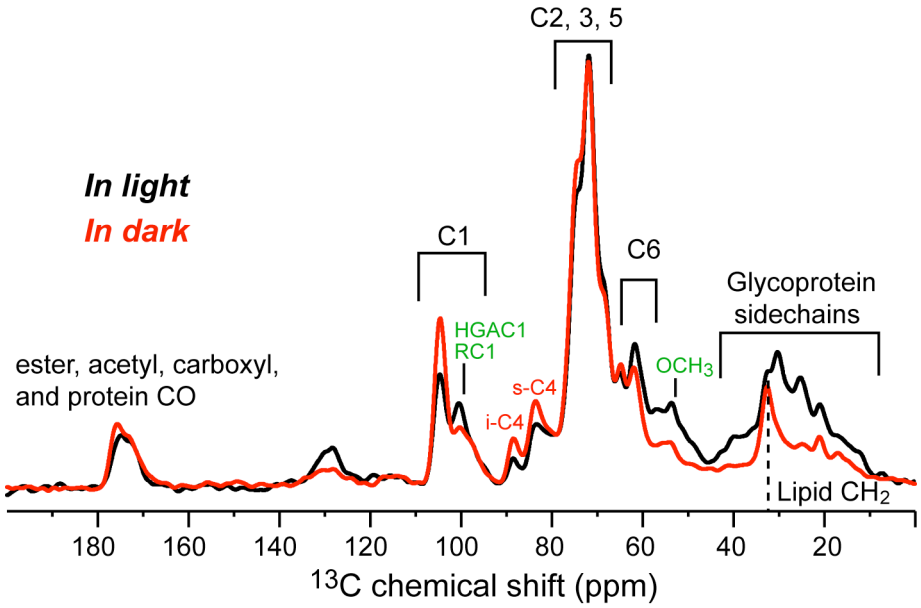

Figure S1. 1D ^{13}C CP-MAS spectra of unlabeled *Arabidopsis* primary cell walls obtained from plants grown in dark (red) versus light (black). The spectra were measured at 253 K under 6 kHz MAS on a 400 MHz NMR spectrometer. Note the similarity of the polysaccharide region of the spectra from 60-110 ppm. Main differences are that the dark-grown cell wall has less protein, less methyl ester (53.5 ppm peak), and slightly less pectins relative to cellulose, as manifested by the weaker 99-ppm peak relative to the 89-ppm peak.

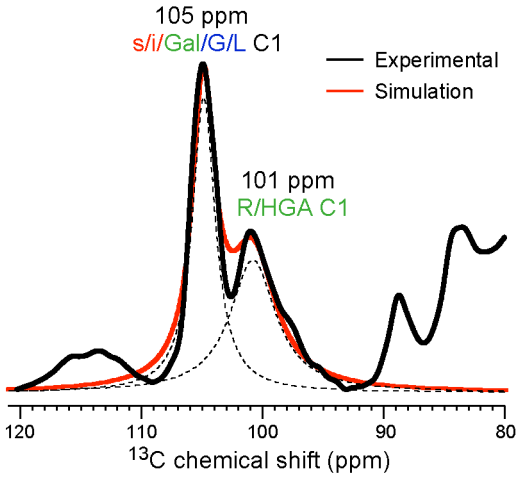

Figure S2. Deconvolution of the 105-ppm and 101-ppm peaks in the 1D ^{13}C CP-MAS spectrum shown in Figure 1. Black: experimental spectrum. Red: sum of the deconvoluted peaks. The deconvolution shows that the upfield wing of the 105-ppm peak contributes only 10% of the total intensity at 101 ppm. For the 105- and 101-ppm peaks, the full width at half maximum are 2.3 and 4.6 ppm, respectively, the relative height is 1 : 0.45 and the relative area is 1 : 0.9.

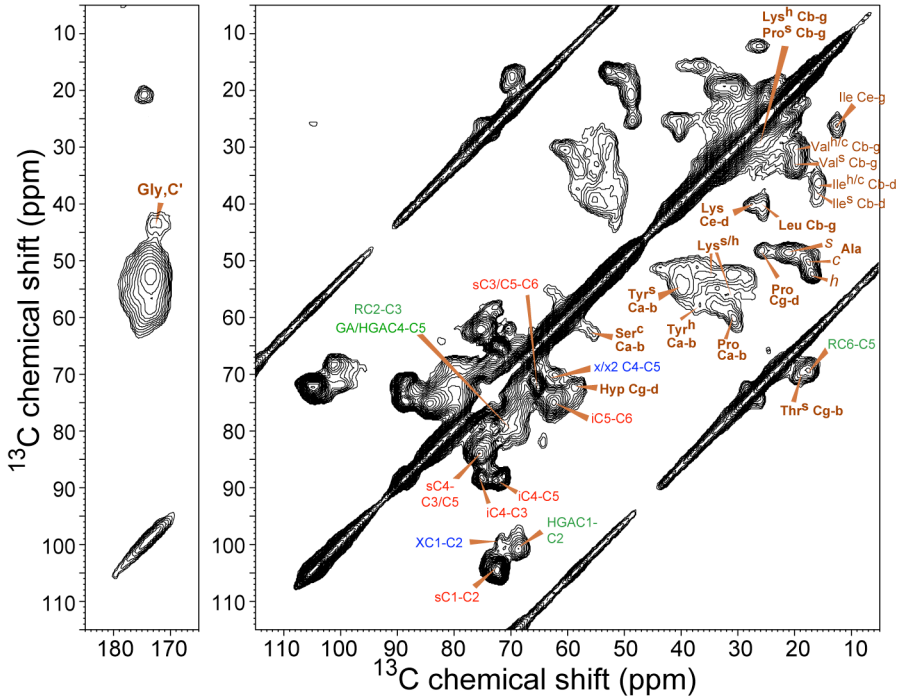

Figure S3. 2D ^{13}C DQ filtered spectrum of ^{13}C-labeled primary cell wall. A Hyp Cγ-Cδ cross peak at (72, 59) ppm is detected.

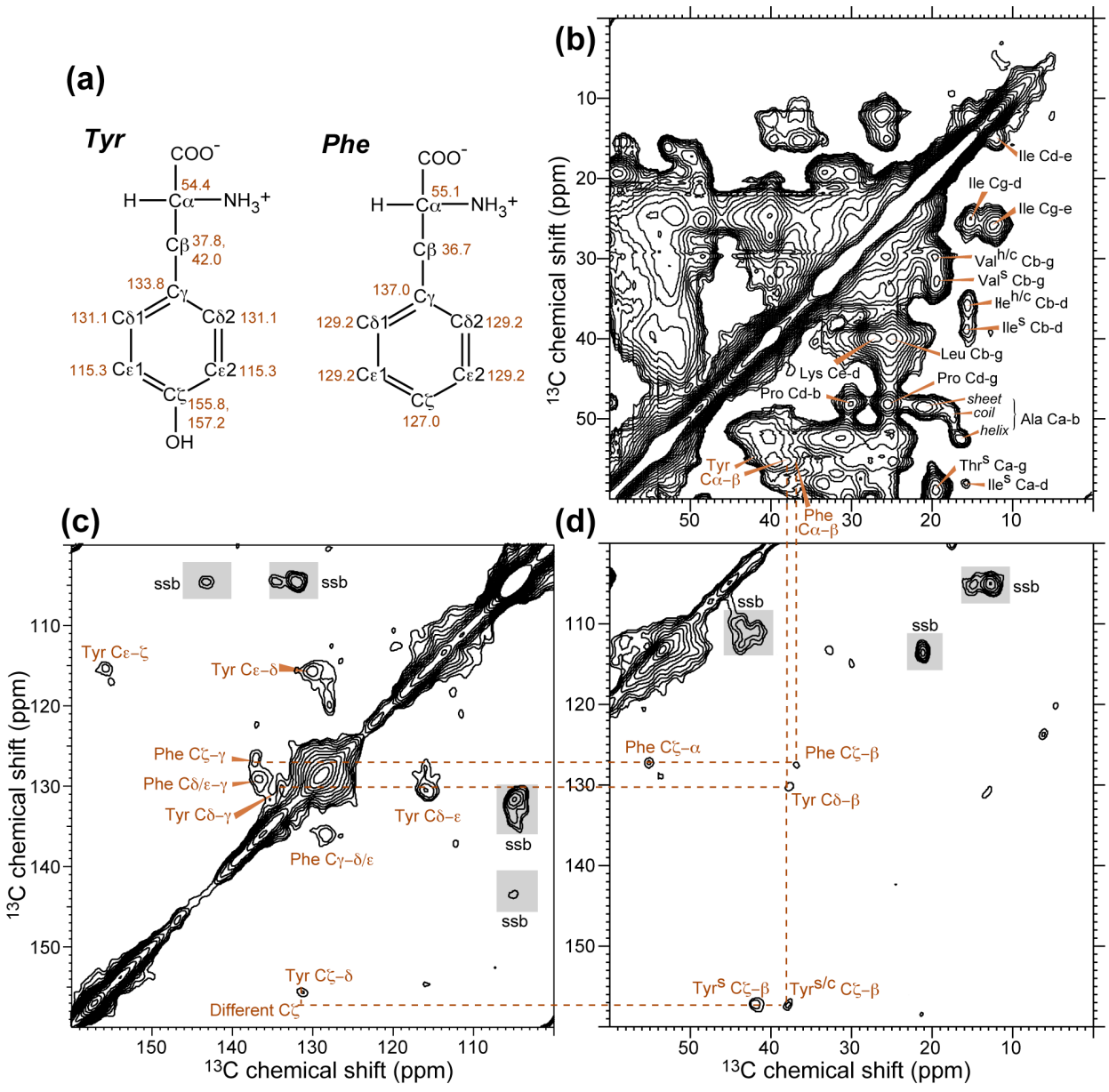

Figure S4. Assignment of Tyr and Phe chemical shifts from the 30-ms ^{13}C PDSD spectrum. (a) Summary of the assigned ^{13}C chemical shifts. (b) Aliphatic region of the 2D spectrum. The area containing the Cα-Cβ peaks of Tyr and Phe shows significant overlap. (c) Aromatic region of the 2D spectrum, showing the Tyr and Phe spin systems. (d) Correlation between aromatic and aliphatic carbons, where two Tyr Cζ-Cβ peaks are observed.

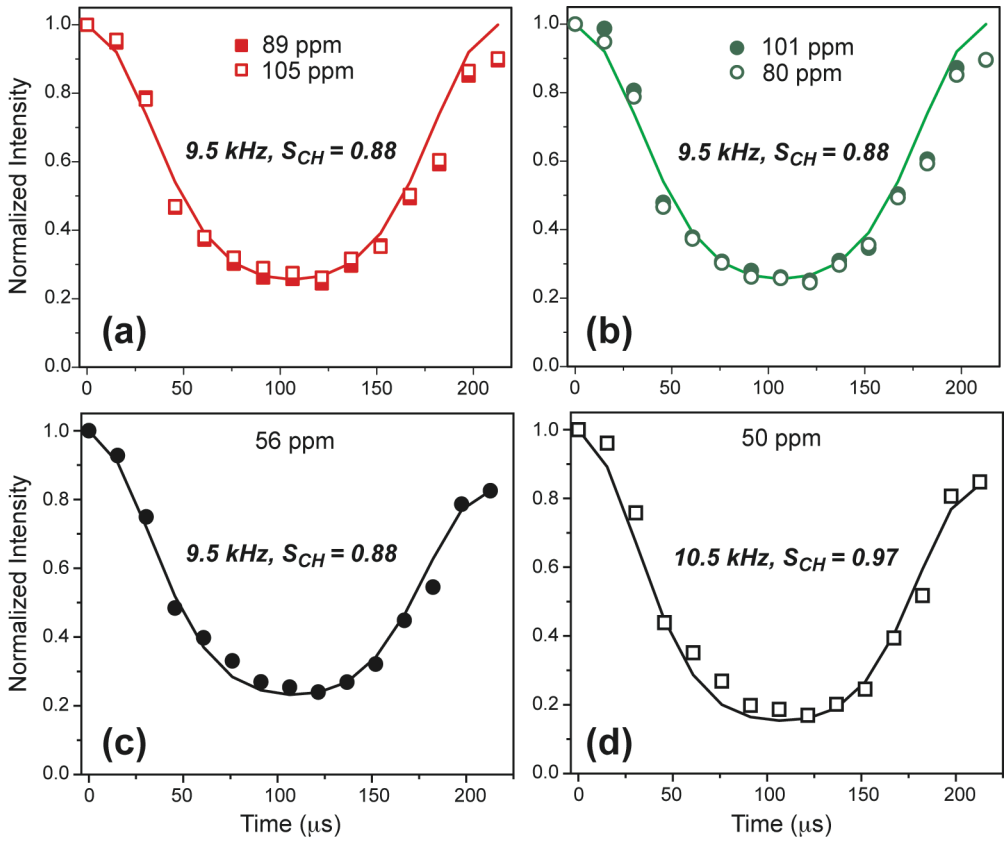

Figure S5. ^{13}C-^{1}H DIPSHIFT spectra of the cell wall at 253 K under 4.7 kHz MAS. (a) Cellulose-rich peaks. 89 ppm: iC4; 105 ppm: i/s/G/Gal C1. (b) Predominantly pectin peaks. 101 ppm: Rha and HGA C1; 80 ppm: Rha C2 and GA C4. (c), (d) Typical protein Cα peaks. 56 ppm: Ser/Phe/Leu Cα; 50 ppm: Ala Cα. For panels (c) and (d), the experimental data show moderate T_2 relaxation, which was simulated using a single exponential decay. The figure shows that cellulose and pectins have similar order parameters S_{CH} of 0.88, indicating similar amplitudes of motion, while the proteins are more rigid at this temperature. Therefore, lack of cross peaks must be attributed to long distances rather than molecular motion.

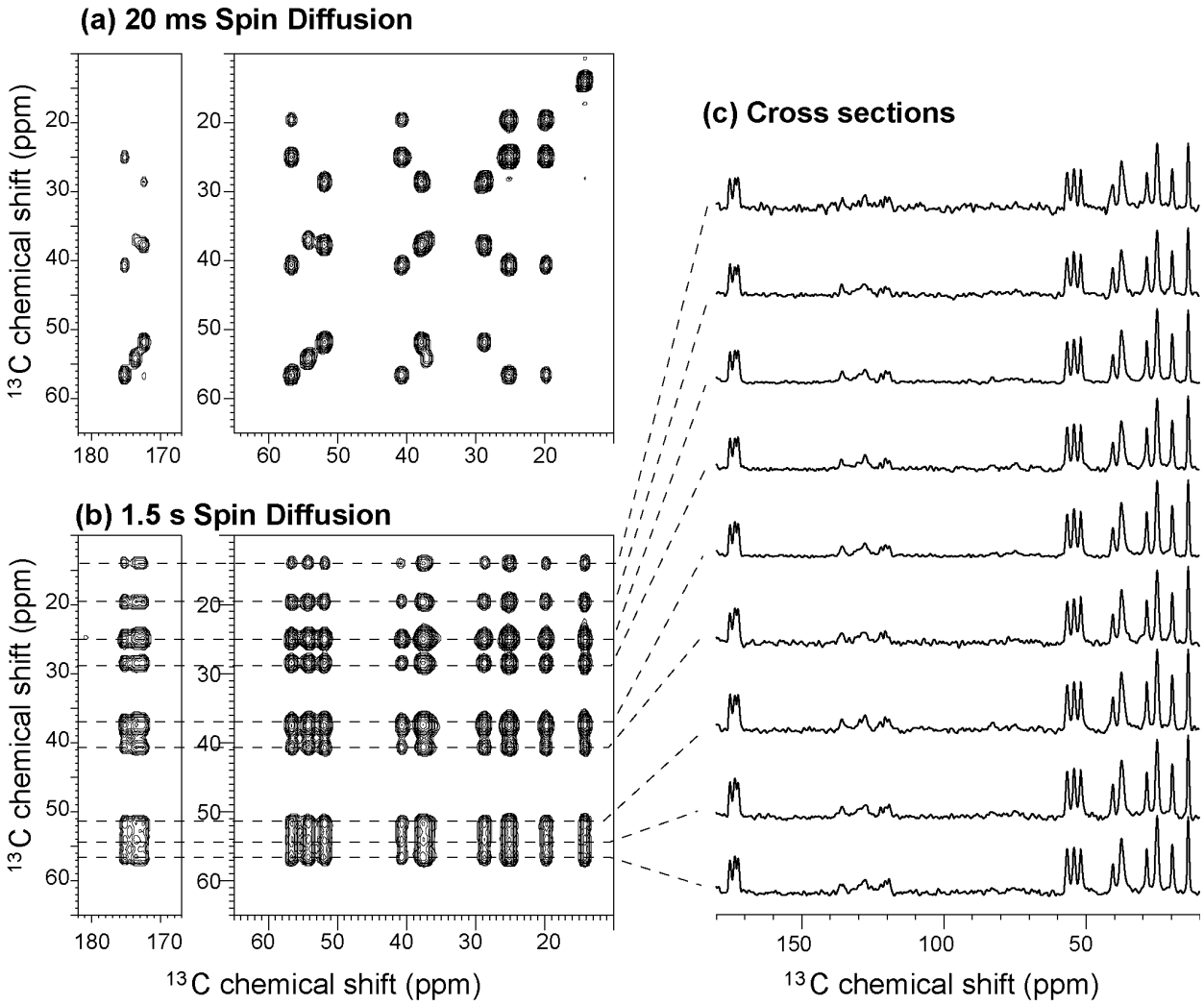

Figure S6. Complete equilibration of ^{13}C magnetization of the tripeptide formyl-Met-Leu-Phe at long spin diffusion mixing times. (a) 20 ms 2D PDSD spectrum. (b) 1.5 s 2D PDSD spectrum. (c) Cross sections of the 1.5 s 2D spectrum show identical intensity patterns for all slices.